RESEARCH/REVIEW ARTICLE

Summer CO_2 evasion from streams and rivers in the Kolyma River basin, north-east Siberia

Blaize A. Denfeld,[1] Karen E. Frey,[1] William V. Sobczak,[2] Paul J. Mann[3] & Robert M. Holmes[3]

[1] Graduate School of Geography, Clark University, 950 Main St. Worcester, MA 01610, USA
[2] Department of Biology, College of the Holy Cross, 1 College Street, Worcester, MA 01610, USA
[3] Woods Hole Research Center, 149 Woods Hole Road, Falmouth, MA 02540, USA

Keywords
Arctic streams and rivers; CO_2 evasion; inland water surface area; Kolyma River; pCO_2; Siberia.

Correspondence
Blaize A. Denfeld, Graduate School of Geography, Clark University, 950 Main St. Worcester, MA 01610, USA.
E-mail: blaize.denfeld@ebc.uu.se

Abstract

Inland water systems are generally supersaturated in carbon dioxide (CO_2) and are increasingly recognized as playing an important role in the global carbon cycle. The Arctic may be particularly important in this respect, given the abundance of inland waters and carbon contained in Arctic soils; however, a lack of trace gas measurements from small streams in the Arctic currently limits this understanding. We investigated the spatial variability of CO_2 evasion during the summer low-flow period from streams and rivers in the northern portion of the Kolyma River basin in north-eastern Siberia. To this end, partial pressure of carbon dioxide (pCO_2) and gas exchange velocities (k) were measured at a diverse set of streams and rivers to calculate CO_2 evasion fluxes. We combined these CO_2 evasion estimates with satellite remote sensing and geographic information system techniques to calculate total areal CO_2 emissions. Our results show that small streams are substantial sources of atmospheric CO_2 owing to high pCO_2 and k, despite being a small portion of total inland water surface area. In contrast, large rivers were generally near equilibrium with atmospheric CO_2. Extrapolating our findings across the Panteleikha–Ambolikha sub-watersheds demonstrated that small streams play a major role in CO_2 evasion, accounting for 86% of the total summer CO_2 emissions from inland waters within these two sub-watersheds. Further expansion of these regional CO_2 emission estimates across time and space will be critical to accurately quantify and understand the role of Arctic streams and rivers in the global carbon budget.

Inland waters are active components of the global carbon (C) cycle storing terrestrially derived C in sediments, transporting large quantities of C from land to the ocean and acting as important regions of C processing and sources of carbon dioxide (CO_2) and methane (CH_4) to the atmosphere. Inland water systems are routinely supersaturated with CO_2 and CH_4 and subsequent C fluxes make them critical components to global atmospheric CO_2 and CH_4 budgets (Kling et al. 1991; Cole et al. 2007; Battin et al. 2009; Aufdenkampe et al. 2011). Headwater streams, comprising a majority of stream length within a given watershed (Bishop et al. 2008), are hotspots of CO_2 concentrations because they interact closely with terrestrial soils and sediment-bound microbes (Hope et al. 2004; Rasera et al. 2008; Teodoru et al. 2009; Davidson et al. 2010; Koprivnjak et al. 2010; Wallin et al. 2010; Butman & Raymond 2011; Benstead & Leigh 2012). Furthermore, headwater streams act as regions of rapid mineralization, processing C exported from terrestrial ecosystems to adjacent rivers and lakes and therefore inclusion of headwater streams is fundamental for accurately quantifying regional CO_2 emissions (Öquist et al. 2009). However, small streams are generally under-represented in global atmospheric CO_2 emission estimates owing to a lack of

Citation: *Polar Research* 2013, *32*, 19704, http://dx.doi.org/10.3402/polar.v32i0.19704

spatial and temporal flux measurements and unquantified areal coverage (Cole et al. 2007; Bishop et al. 2008; Melack 2011; Benstead & Leigh 2012).

CO_2 evasion to the atmosphere from surface waters is jointly controlled by the partial pressure of carbon dioxide (pCO_2) and the gas exchange velocity (k) of CO_2 at the water–atmosphere interface. Terrestrially derived C greatly influences riverine pCO_2, entering either as dissolved inorganic carbon (DIC) directly in the form of CO_2 from soil respiration, decomposition and weathering of bedrock minerals, or as dissolved organic carbon (DOC) from allochthonous organic C that can subsequently be respired within the stream (Butman & Raymond 2011 and references within). In addition, autochthonous organic C produced in the stream (e.g., emergent macrophytes) reduces pCO_2 via photosynthesis and increases pCO_2 via respiration. As organic C is transported downstream, microbial respiration and phototransformation may alter the lability of C, potentially affecting its degradability (Aufdenkampe et al. 2011; Mann et al. 2012). Furthermore, across a river network the DOC (Laudon et al. 2011) and DIC (Tank et al. 2012) entering inland waters can vary seasonally as the hydrograph transitions from spring freshet to late summer flow conditions (Neff et al. 2006; Holmes et al. 2008; Holmes et al. 2012).

Rapid CO_2 evasion has been found to occur in headwater streams (Öquist et al. 2009) as high water turbulence increases the exchange ability of CO_2 at the water–atmosphere interface (Raymond et al. 2012). As streams become wider and deeper, gas exchange velocities become increasingly influenced by wind-driven processes, rather than turbulent flow processes (Alin et al. 2011). Gas exchange velocities can therefore vary spatially within a watershed (Alin et al. 2011; Raymond et al. 2012), owing to differences in sub-watershed climate, land cover and morphology. Consequently, CO_2 evasion in permafrost-dominated rivers likely varies spatially and seasonally across river networks, yet to this point has not been systematically quantified across these important landscapes.

Past studies focused on inland water CO_2 evasion have been conducted in tropical regions of the Amazon (Richey et al. 2002; Rasera et al. 2008; Davidson et al. 2010), temperate regions (Hope et al. 2001; Jones et al. 2003; Butman & Raymond 2011), boreal regions (Kelly et al. 2001; Teodoru et al. 2009; Koprivnjak et al. 2010; Wallin et al. 2010), and the Alaskan Arctic (Kling et al. 1991; Cole et al. 1994); however, CO_2 evasion from lotic systems in the Siberian Arctic has not yet been reported. Arctic landscapes are critical for understanding global CO_2 emissions from inland water surfaces as permafrost occupies about 22% of the exposed land surface in the Northern Hemisphere (Zhang et al. 1999), which if thawed will likely release an old and potentially labile source of C to streams (Frey & McClelland 2009). Permafrost, storing large quantities of long-sequestered soil C (Zimov et al. 2006), plays a unique role in the hydrologic pathways of terrestrially derived C entering inland waters by minimizing percolation into deep soils (Frey et al. 2007). In permafrost-dominated regions, terrestrially derived C enters streams via surface and shallow surface pathways with minimal ground water flow, even during summer periods.

This study focuses upon CO_2 evasion from headwater (order 1–3) streams to the Kolyma River main stem, exploring the spatial variability in riverine pCO_2 and gas exchange velocities during summer low-flow conditions. Additionally, DOC concentration and five-day biological oxygen demand (BOD) were measured to help interpret spatial patterns in pCO_2. The objectives of this study were to: (a) determine pCO_2 concentrations for individual streams and rivers in a permafrost-dominated riverine system within the northern Kolyma River basin during the summer low-flow period; (b) understand the spatial variability of CO_2 evasion fluxes from streams and rivers across this region; and (c) estimate total CO_2 emission from sub-watersheds as a whole within the northern Kolyma River basin (requiring the areal coverage of streams and rivers to be quantified). To address these objectives, field-based measurements of summer pCO_2 and gas exchange velocities were combined with geographic information system (GIS) and remote sensing techniques to extrapolate summer CO_2 flux estimates across a bounded study area in the northern Kolyma River basin region, as well as two sub-watersheds within the region (the Panteleikha–Ambolikha river watershed).

Data and methods

Study site

The Kolyma River basin in north-east Siberia is the largest Arctic watershed (ca. 650 000 km^2) completely underlain by continuous permafrost. The major soils in this region, known as yedoma, store vast amounts of sequestered organic C and nutrients, characterized by Pleistocene-aged, ca. 10–90 m thick icy loess deposits containing ca. 3–5% organic C (Zimov et al. 2006). The soils are comprised of a shallow organic top layer (ca. 5–7 cm) underlain by permafrost, with active layer thicknesses that range from ca. 50 to 90 cm. The bedrock in this region retains a relatively large proportion of basalts compared to other large Arctic watersheds and therefore carbonate (ca. 78–85%) and silicate (ca. 22–42%) weathering both contribute to the inorganic C pool

Citation: *Polar Research* 2013, *32*, 19704, http://dx.doi.org/10.3402/polar.v32i0.19704

in the region (Tank et al. 2012). The diverse forest–tundra vegetation and mountain–floodplain landscape (Semiletov 1999) combined with strong continental climate of warm summers (mean ca. 12°C), cold winters (mean ca. −35°C) and low annual precipitation (mean ca. 185 mm yr^{-1}; Welp et al. 2005) promote seasonally variable river discharge. Annual discharge in the Kolyma River (mean ca. 132 km^3) follows a seasonal hydrological pattern typical of Arctic rivers, with a sharp rise and fall in discharge during the spring freshet and consistently low winter discharge (Holmes et al. 2012).

Sampling pCO_2 during summer low flow

From 11 July to 14 August 2010, during summer low-flow conditions, a survey spanning ca. 260 km of the northern region of the Kolyma River was conducted to examine biogeochemical properties among a diverse set of river locations and tributaries. A total of 29 different sites were sampled (10 stream, 11 river, and eight Kolyma main stem locations), 14 of which were sampled two or more times (total $n = 56$; Fig. 1). For the purpose of this study, "streams" were defined where total reach length was <10 km and "rivers" were defined where total reach length was >10 km. Reach length refers to the length from a stream or river source (headwater streams from lake/wetland source and higher order streams from the confluence of the connecting water body upstream) to the outlet (defined as the point of confluence into another water body). At each location, pH, temperature, dissolved oxygen (DO) saturation and specific conductivity were measured using a Pro Plus multiparameter instrument (YSI, Yellow Springs, OH, USA) at a depth of ca. 0.5 m (Table 1). In shallow streams, less than 0.5 m in depth, measurements were taken approximately midway below the surface and the bottom. Water samples for DOC and pCO_2 were collected in dark bottles without headspace to minimize degassing. Upon returning from the field, DOC samples were filtered through precombusted 0.7-μm GF/F glass fibre filters (Whatman, Kent, UK) directly into acid-washed, precombusted glass vials and acidified with HCl to a pH of <2, following the protocol used by Mann et al. (2012). Samples were refrigerated in the dark until measurement (within one week of collection) at the Northeast Science Station (Cherskiy, Russia) via high-temperature combustion using a TOC-V organic carbon analyzer combined with nitrogen detection unit (TNM-1) (Shimadzu Scientific Instruments, Columbia, MD, USA) (0.5 μg L^{-1} detection limit). DOC was calculated as the mean of ca. 3–5 injections with a coefficient of variance always <2%. Samples for alkalinity analyses were filtered through 0.45-μm Sterivex-HV filters (Millipore, Watford, UK) and were analysed within one day of collection. Total alkalinity was determined using a digital titrator (Hach, Loveland, CO, USA) using the Gran function plot method in an alkalinity calculator (http://or.water.ursgs.gov/alk/). Carbonate alkalinity was calculated by correcting for organic anion contributions to total alkalinity, using measured DOC and pH (Thurman 1985). Briefly, organic anion contributions were calculated as the percent fulvic DOC dissociated in water, assuming that 90% of the measured DOC was fulvic. pCO_2 was then calculated from carbonate alkalinity, pH, water temperature and temperature-adjusted dissociation constants for carbonic acid (K_1 and K_2; Millero 2010) and water (K_W; Millero 1979).

The following equation utilized for determining pCO_2 was adapted from Stumm & Morgan (1981):

$$pCO_2 = \frac{\left(\frac{(\mathrm{Alk} - [\mathrm{OH}^-] + [\mathrm{H}^+])}{(\alpha_1 + 2\alpha_2)}\right)\ (\alpha_0),}{K_0} \qquad (1)$$

where pCO_2 (in units of microatmospheres [μatm]) does not directly refer to the concentration of free CO_2 in water but rather—applying Henry's Law of gas constant (K_o)—suggests that the concentration of a dissolved gas is proportional to its pressure in the gas phase. K_o, expressed in mol L^{-1} atm refers to a litre of solution at the temperature of the measurement (Weiss 1974). Carbonate species relation equations ($\alpha_0 = H_2CO_3$, $\alpha_1 = HCO^{3-}$, $\alpha_2 = CO_3^{2-}$), referenced from Stumm & Morgan (1981), account for the activity of each individual carbonate species. At select locations—streams ($n = 8$), rivers ($n = 10$), main stem ($n = 4$)—60-mL HDPE bottles were slowly filled with water to be analysed in the laboratory for BOD. BOD was calculated as the difference in DO concentration (mg L^{-1}) before and after five-day incubations of unfiltered waters in the dark at room temperature (20°C).

Finally, discharge data for the Kolyma River at Kolymskoye were obtained from the ArcticRIMS database and adjusted to reflect discharge of the Kolyma River at Cherskiy, located about 160-km downstream of the Kolymskoye gauging station (e.g., Holmes et al. 2012). Daily discharge data (Fig. 2) for the Kolyma River were used to assist in understanding summer low-flow hydrology and potential influences on biogeochemistry within this region.

Gas exchange velocity (k) measurements

CO_2 flux estimates require an understanding of k, which varies as a function of physical and environmental

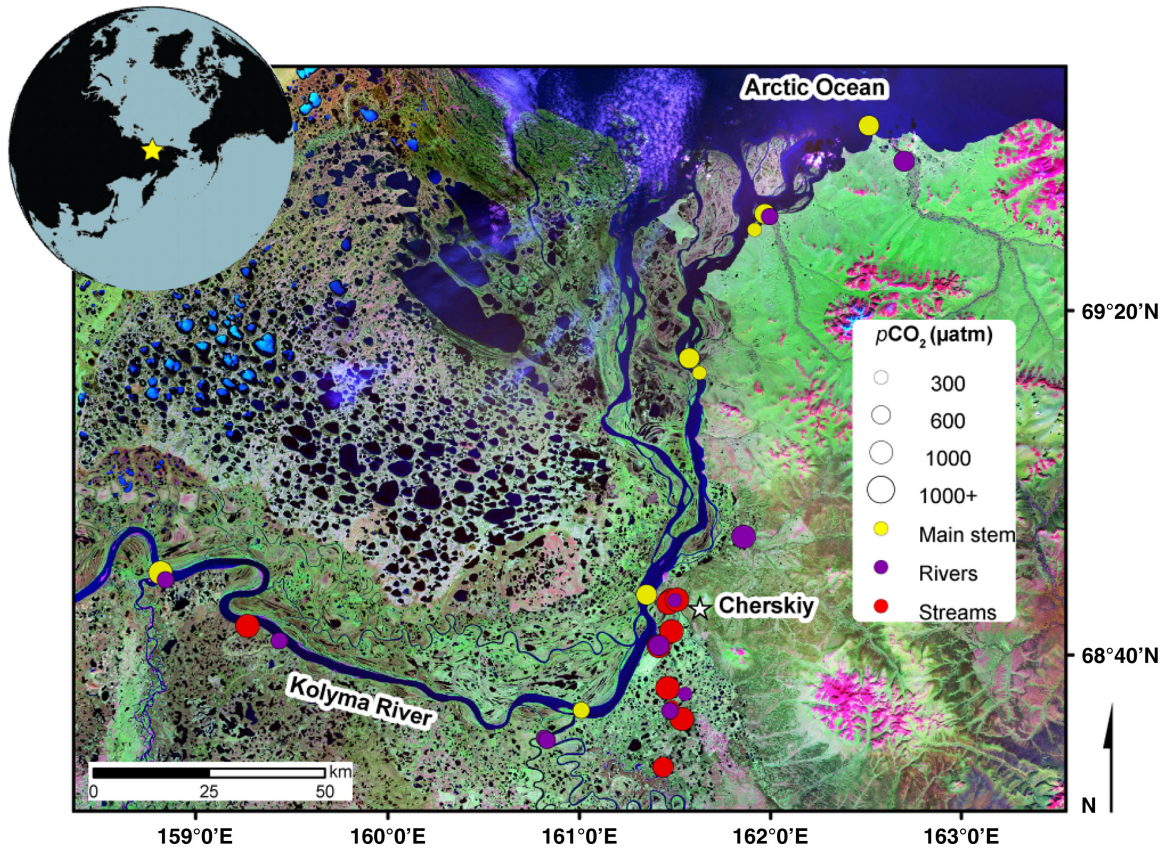

Fig. 1 Field sample locations from 11 July to 14 August 2010. A total of 29 different sites were sampled (10 stream, 11 river and eight main stem locations), 14 of which were sampled two or more times (total $n = 56$) spanning ca. 260 km along the Kolyma River main stem. Aquatic system types are colour coded, and streams and rivers were defined where reach length was <10 km and >10 km, respectively. Average pCO_2 for each site is represented by varying circle size.

characteristics of the system (Alin et al. 2011). Several recent studies have utilized values for k from the literature without empirical field validation (e.g., Teodoru et al. 2009; Humborg et al. 2010), yet direct measurements of k allow for more accurate CO_2 evasion estimates (Wallin et al. 2011). One such field approach utilizing floating chambers offers a highly localized measurement of k. The chamber method has been criticized for potentially reducing wind shear, causing mass boundary layer perturbations, or disturbing the air–water interphase, yet there is no consensus about whether fluxes measured by chambers yield values consistent with other methods (Alin et al. 2011) or overestimates compared to other methods (Vachon et al. 2010). However, due to the remote region of our study, floating chambers offered a relatively robust approach for directly measuring k for a diverse set of stream and rivers.

During the summer of 2011, we measured the evasion of pCO_2 across the air–water interface to assess k values across streams ($n = 8$), rivers ($n = 8$) and the Kolyma main stem ($n = 3$). We traced the accumulation of CO_2 in a circular, plastic chamber with a fixed headspace. The chamber (30 cm above water level) was allowed to float freely along streams or alongside a boat to minimize interference from water turbulence. The concentration of CO_2 was continually monitored using a closed air circuit and air-pump flowing through a GM70 portable infrared gas analyser system (Vaisala, Vantaa, Finland). Values of k were calculated from the slope of the linear regression of pCO_2 over a 15-min deployment time (with r^2 values typically greater than 0.98). Values of k were then calculated in units of cm hr^{-1}. To compare gas transfer velocity values among sites and aid in comparison with other studies, k values were normalized to a temperature of 20°C using a Schmidt number of 600, that is, k_{600} (e.g., Alin et al. 2011).

CO_2 evasion flux calculations

To calculate CO_2 evasion fluxes (g C m^{-2} d^{-1}), the rate that CO_2 degasses from surface waters to the atmosphere, the following equation was utilized:

Citation: *Polar Research* 2013, *32*, 19704, http://dx.doi.org/10.3402/polar.v32i0.19704

Table 1 Summary description of physical and biogeochemical characteristics of streams (<10 km reach length) and rivers (>10 km reach length) sampled in the northern Kolyma River basin during summer low-flow conditions.

		Physical characteristics[a]					Biogeochemical characteristics						
Inland water type	Range	Watershed (km^2)	Reach length (m)	Width (m)	Slope (°)	k^b (cm h^{-1})	Temp (°C)	DO[c] (% sat.)	Cond[d] (µS cm^{-1})	pH	DOC[e] (mg L^{-1})	Alk[f] (µeq L^{-1})	pCO_2^g (µatm)
Streams (n = 21)	Min	0.03	152	1	0.2	3	4.5	33	110	6.44	5.0	0.28	274
Reach length <10 000 m	Max	17	5403	19	6.5	55	19.0	114	41	7.82	21.6	1.36	9402
	Mean	5	2051	7	3.1	21	13.1	73	67	7.04	13.8	0.63	3336
Rivers (n = 21)	Min	59	19 389	23	0.9	5	11.5	22	92	6.92	2.0	0.09	5
Reach length >10 000 m	Max	115 166	815 447	400	6.5	37	20.5	119	21	9.13	11.5	0.69	1010
	Mean	23 115	222 284	158	2.1	16	16.0	89	50	7.69	5.5	0.27	412
Kolyma River (n = 14)	Min	424 505	2 024 530		1.6	8	11.8	88	129	7.47	3.2	0.39	123
	Max	664 119	2 319 608		1.8	28	20.1	106	66	8.22	5.3	0.81	1079
	Mean	630 029	2 232 463		1.7	17	16.1	94	88	7.75	4.4	0.56	613

[a]Sample size (n) only includes individual watershed once; streams (n = 19), rivers (n = 11), main stem (n = 8).
[b]Based on samples collected during summer 2011; streams (n = 8), rivers (n = 9), main stem (n = 3).
[c]Dissolved oxygen.
[d]Conductivity.
[e]Dissolved organic carbon.
[f]Alkalinity.
[g]Partial pressure of carbon dioxide.

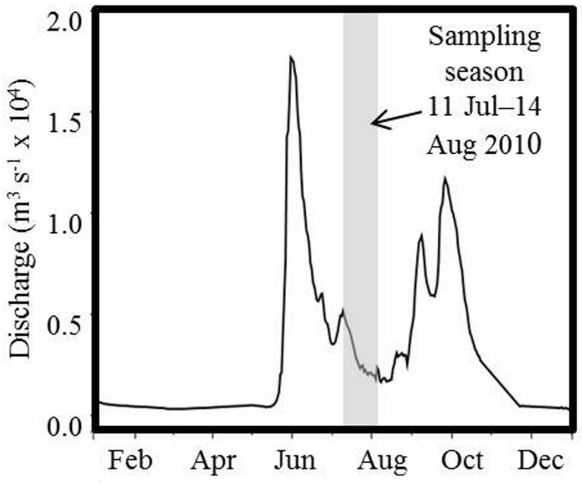

Fig. 2 Daily discharge of the Kolyma River (adjusted to Cherskiy, Russia, ca. 160 km downstream of the gauging station at Kolymskoye) for 2010. The grey box indicates the sampling season of this study (11 July–14 August 2010), representing summer low-flow conditions.

$$\text{Evasion flux}_{(CO_2)} = k * k_h(pCO_{2\ \text{water}} - pCO_{2\ \text{air}}), \quad (2)$$

where average k values were used for streams, rivers and the Kolyma main stem (21.2 cm hr^{-1}, 16.2 cm hr^{-1},16.7 cm hr^{-1}, respectively); k_h (Henry's constant) corrects for temperature (Weiss 1974); ($pCO_{2\ \text{water}} - pCO_{2\ \text{air}}$) accounts for the difference between concentrations in the water and in the air; and $pCO_{2\ \text{air}}$ (the atmospheric CO_2 concentration) was set to 389.3 ppm, the average global 2010 atmospheric CO_2 concentration during the sampling period (11 July–15 August) (Tans & Keeling undated).

Areal CO_2 emission calculations

To obtain estimates of areal CO_2 emissions (g C d^{-1}) from inland surface waters, CO_2 evasion fluxes (Eqn. 2) were multiplied by surface water area estimates. Regional estimates of CO_2 emission from inland water bodies rely as much on estimates of inland surface water area as on the CO_2 evasion per unit area of surface water (Aufdenkampe et al. 2011), emphasizing the importance of accurately quantifying surface water area. Owing to the expansive and remote nature of north-east Siberia, GIS techniques and satellite remote sensing offer powerful and practical tools to determine surface water area, providing a means to extrapolate pCO_2 field measurements beyond field-based sampling sites alone and allowing for areal CO_2 emissions to be calculated.

To determine areal CO_2 emissions, both CO_2 evasion fluxes from non-sampled stream and river surface areas needed to be estimated. Since the Kolyma River network comprises a few large rivers and a vast amount of small

streams and rivers, four different data sets were utilized to represent the varying spatial scales of our field-based sampling sites (Fig. 3, Table 2). Satellite imagery was acquired during summer, allowing surface area conditions to be accurately determined during typical low-flow conditions. All satellite imagery was geometrically corrected and georeferenced to UTM zone 57N. Watershed area and Kolyma main stem surface area were manually digitized from orthorectified Landsat Thematic Mapper mosaics. A threshold classification technique was applied to Phased Array type L-band Synthetic Aperture Radar (PALSAR) and GeoEye imagery to determine surface areas for rivers and larger streams (i.e., streams that were detectable in this imagery). Imagery was reclassified as water and non-water based on empirically determined pixel value histograms (e.g., Smith & Alsdorf 1998). However, the smallest streams sampled in this study were not readily apparent in GeoEye imagery owing to such conditions as thickly vegetated overstories. A digital elevation model (DEM) can provide a more detailed picture of smaller channels that are often undetectable by traditional mapping techniques (Benstead & Leigh 2012). As such, through topographic modelling of stream networks (with the use of Hydrological Extension in ESRI® ArcGIS™ v. 10.0 software), Advanced Spaceborne Thermal Emission and Reflection Radar DEM data allowed for

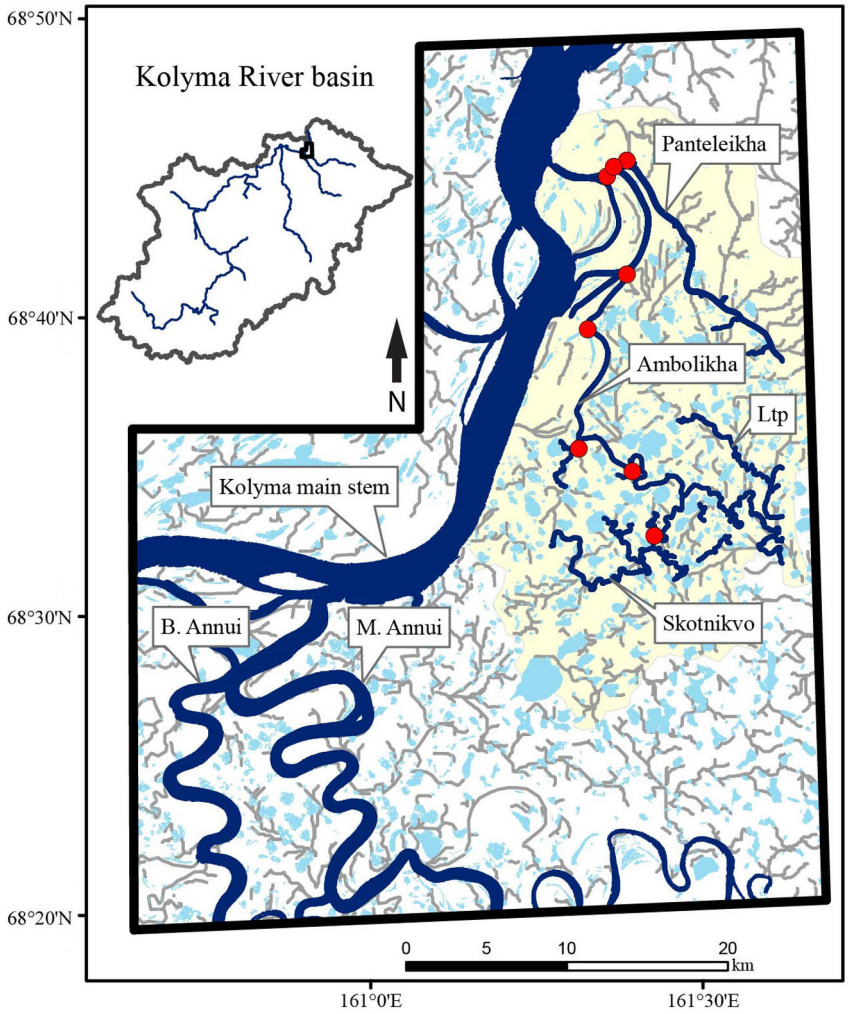

Fig. 3 Bounded study area of the lower Kolyma River basin (black box). Areal coverage of surface water for a subset of sampled rivers and streams in the Kolyma River basin determined using four different types of satellite remotely sensed imagery (Table 2). Dark blue determined from pixel value histogram reclassification and light grey predicted from the ArcGIS™ Hydrological Extension (Table 3). Light yellow area represents the portion of the Panteleikha–Ambolikha watershed covered by GeoEye imagery (30% of the total watershed areas; Table 4). Red dots denote sampled stream locations. Lakes (light blue) were included for clarity.

Citation: *Polar Research* 2013, *32*, 19704, http://dx.doi.org/10.3402/polar.v32i0.19704

Table 2 Summary of satellite imagery used to determine water surface area within the bounded study area.

Data set	Acquisition date	Spatial resolution	Spatial coverage of study area	Availability
Orthorectified Landsat Thermatic Mapper Mosaic	N/A	14.25 m	Kolyma River main stem	National Aeronautical and Space Administration Applied Science and Technology Project Office http://zulu.ssc.nasa.gov/mrsid/
Phased Array type L-band Synthetic Aperture Radar (PALSAR)	30 July 2010	12.755 m	Large rivers (M. and B. Annui)	Alaska Satellite Facility http://www.asf.alaska.edu/
GeoEye (Panchromatic)	13 August 2009	0.48 m	Small rivers[a] and streams	GeoEye http://geofuse.geoeye.com/maps/Map.aspx
Advanced Spaceborne Thermal Emission and Reflection Radar Digital Elevation Model	N/A	15 m	Length of small streams (order 1–3)	Earth Observing System Data and Information System. 2009. https://wist.echo.nasa.gov/api/

[a]Small rivers were those that PALSAR had difficulty characterizing because of their smaller size but instead could be identified in GeoEye.

the smallest streams (order 1–3; not identified with the GeoEye imagery) to be represented (at stream lengths >200 m). Stream surface area was determined by multiplying stream length (an output of Hydrological Extension) and width (determined from an empirical relationship), where the following empirical relationship with length provided the best prediction of stream width: (width $=0.0018$ [length]; $r^2=0.91$, $n=12$, $p<0.001$). The sample size ($n=12$) in this relationship represented the eight streams and four rivers whose total length and width (orthogonal distance across the inundated area) was determined from the PALSAR and GeoEye imagery acquired during summer low-flow conditions.

CO_2 evasion fluxes were then estimated from non-sampled streams in the riverine network using an empirically derived relationship to predict pCO_2 for non-sampled streams from field-based pCO_2 and averaged k (calculated as 21.2 cm hr^{-1}) for streams. The empirical relationship with stream width ($pCO_2 = 3739.2e^{-0.118[width]}$, $r^2=0.63$, $n=8$) provided the best relationship for predicting pCO_2. This relationship only includes stream samples ($n=8$)—and excludes river samples—for two reasons: (1) pCO_2 in streams are highly variable compared to river samples; and (2) non-sampled streams were of lengths (<10 km) and widths (<20 m) most comparable to the range of our sampled streams.

Using the relationships determined above, areal CO_2 emission was then determined within a bounded study area (e.g., Teodoru et al. 2009), defined by the available remotely sensed imagery of the northern Kolyma River basin (Fig. 3). Next, values were extrapolated to a watershed boundary providing a more meaningful and systematic approach to upscaling. An extrapolation to the entire Kolyma River basin would require an increased number of watersheds represented in the southern and mid-Kolyma River basin at much lower latitudes; therefore, logistical and analytical constraints limited extrapolation to sub-watersheds in the northern region of Kolyma River only. The Panteleikha–Ambolikha watershed was selected for this analysis because they were highly sampled within our study area, including eight streams, two rivers, and the Ambolikha and Panteleikha main stems. Landsat imagery covers 100% of these two watersheds; however, fine resolution GeoEye imagery only covers 30% of the two watersheds. As such, the total length of the Panteleikha River was manually determined and the average width was applied to obtain the total Panteleikha main stem surface area. For all other rivers and streams in the two watersheds, the proportion of total stream and river surface area in the known 30% area of watershed was applied to the total area of the watershed.

Results

Spatial patterns of CO_2 evasion during summer low flow

Physical and biogeochemical characteristics among riverine system types exhibited wide variability (Table 1); streams had the lowest pH (mean 7.04 ± 0.38), whereas rivers (mean 7.69 ± 0.60) had slightly higher pH values than the main stem (mean 7.75 ± 0.21). Sampling sites had low, yet variable, alkalinity (ranging from ca. 0.09 to 1.36 μeq L^{-1}), with extremely low values recorded in rivers (mean ca. 0.21 μeq L^{-1}). Overall, streams were consistently supersaturated in CO_2 (excess partial pressure of carbon dioxide [$EpCO_2$] 2948 μatm), while rivers ($EpCO_2$ 24 μatm) and the Kolyma main stem were slightly supersaturated in CO_2 ($EpCO_2$ 225 μatm). pCO_2 was high in streams (mean 3336 ± 2737 μatm) compared to rivers (mean 412 ± 250 μatm) and the Kolyma main stem (mean 613 ± 315 μatm; Fig. 4a). Values of k were

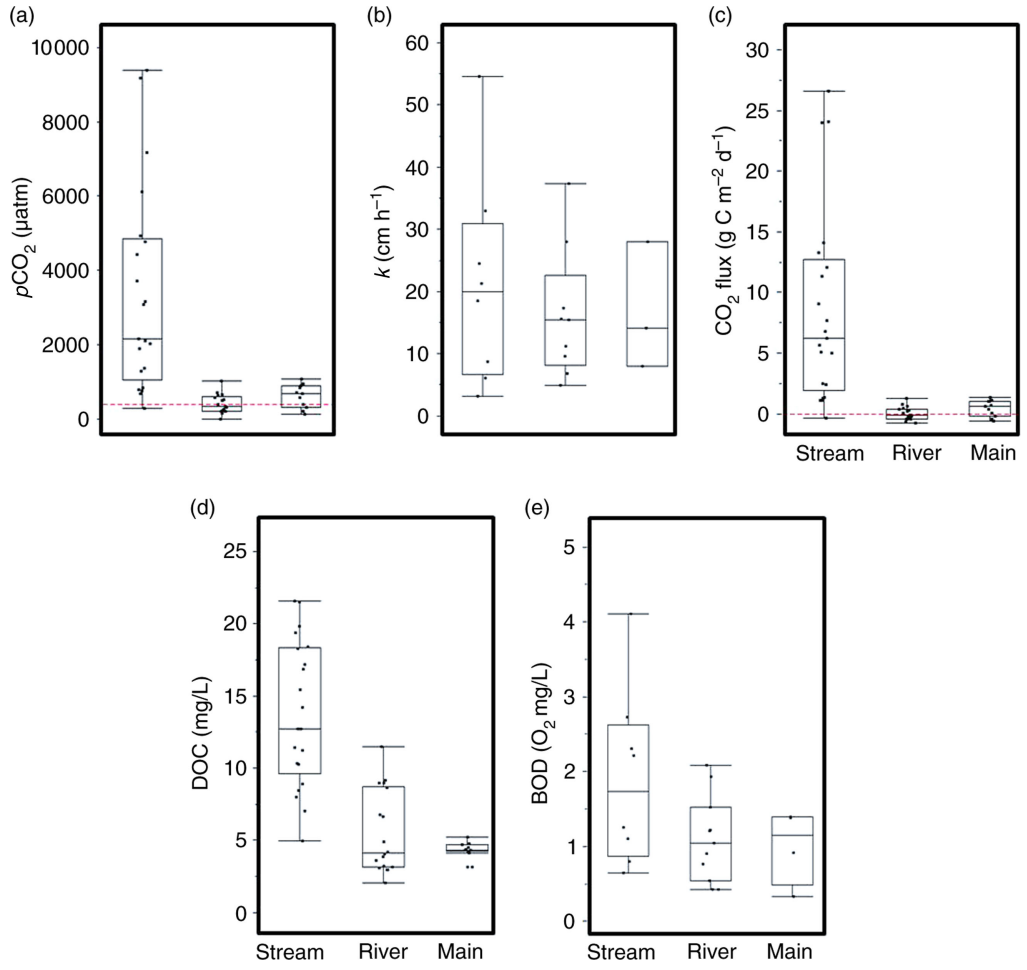

Fig. 4 Comparison of (a) pCO_2 (µatm), (b) k (cm hr^{-1}), (c) CO_2 flux (g C m^{-2} d^{-1}), (d) dissolved organic carbon (DOC, in mg L^{-1}) and (e) biological oxygen demand (BOD, in mg L^{-1}) among streams (<10 km reach length), rivers (>10 km reach length) and the Kolyma main stem. Box plots show range, quartiles and median. The red dashed line in (a) represents 389.3 µatm, the mean 2010 atmospheric CO_2 concentration during the sampling period (11 July–14 August 2010) and the red dashed line in (c) represents CO_2 in equilibrium with the atmosphere (values above the line indicate a CO_2 source and values below the line indicate a CO_2 sink). Average k for streams, rivers and Kolyma main stem (21.2 cm hr^{-1}, 16.2 cm hr^{-1}, 16.7 cm hr^{-1}, respectively) were used to calculate CO_2 flux.

variable among streams (mean 21.2 ± 16.8 cm hr^{-1}), rivers (mean 16.2 ± 10.5 cm hr^{-1}) and the Kolyma main stem (mean 16.7 ± 10.3 cm hr^{-1}; Fig. 4b). CO_2 evasion fluxes followed a similar pattern to pCO_2 and k, with highly variable fluxes from streams (mean 8.6 ± 8.0 g C m^{-2} d^{-1}) compared to rivers (mean 0.007 ± 0.5 g C m^{-2} d^{-1}) and the Kolyma main stem (mean 0.5 ± 0.7 g C m^{-2} d^{-1}; Fig. 4c). DOC concentration and variability decreased along the fluvial path from streams (mean 13.8 ± 5.0 mg L^{-1}) to rivers (mean 5.5 ± 2.9 mg L^{-1}) to the main stem (mean 4.4 ± 0.5 mg L^{-1}; Fig. 4d). Mean BOD rates declined moving from streams (mean 1.9 ± 1.2 mg L^{-1}), rivers (mean 1.1 ± 0.6 mg L^{-1}) and the Kolyma main stem (mean 1.0 ± 0.5 mg L^{-1}; Fig. 4e).

To address hydrologic and watershed processes within the stream category, streams were separated depending upon source material loading categories: (a) yedoma streams (draining upland high C-content yedoma soils); (b) floodplain streams (draining low-lying terrestrial vegetation and Holocene soils) and (c) connecting streams (linking a confluence of lakes and wetlands). Yedoma streams were typically long (mean 3562 ± 1903 m length) and narrow (mean 2.0 ± 1.4 m width); floodplain streams were usually more narrow (mean 2.0 ± 0.0 m width) within small watersheds (mean 0.5 ± 0.8 km^2 watershed area); and connecting streams were relatively long (mean 2156 ± 2190 m length) and wide (mean 14.0 ± 4.5 m width). Yedoma streams typically contained

Citation: *Polar Research* 2013, *32*, 19704, http://dx.doi.org/10.3402/polar.v32i0.19704

highest DOC concentrations (mean 18.0 ± 2.5 mg L^{-1}), yet floodplain streams had highest pCO_2 (mean 4661 ± 2990 µatm). In contrast, connecting streams had the lowest DOC concentrations (mean 8.0 ± 0.4 mg L^{-1}) and pCO_2 (mean 775 ± 1192 µatm).

Areal CO_2 emission estimates

Areal CO_2 emission was calculated within a bounded study area, defined by the available remotely sensed imagery of the northern Kolyma River basin (Fig. 3; Table 3). The drainage network within the defined study area covers a total of 9.3% of the defined study area (1871 km^2), composed of 1034 streams (order 1–3), four small rivers (Skotnikvo, Ambolikha, Panteleikha, Ltp), two large tributary rivers (Bolshoi Annui and Malinki Annui) and the Kolyma River main stem, representing 0.2, 0.3, 1.6 and 7.2% of the defined study area, respectively. Streams (order 1–3) comprise a majority of stream length but contribute only a small fraction of total inland water surface area (ca. 2.4%). To calculate areal CO_2 emission, k values averaged for each system type (Table 1) were used. The areal CO_2 emission for the summer low-flow period from the combined stream–river–main stem network within the bounded study area was ca. 75.5×10^6 g C d^{-1}, ca. 38.3% of which was emitted by streams, ca. 0.4% by small rivers and ca. 61.3% by the Kolyma River main stem alone. In contrast, large rivers on average acted as a weak CO_2 sink, reducing the areal emission of CO_2 by ca. 2.0%.

To broadly investigate the fractional CO_2 contribution from inland waters in the Kolyma River basin from a watershed perspective (as opposed to an arbitrary bounded study region, as above), values from the northern Kolyma River defined study zone (Fig. 3) were additionally scaled to the Panteleikha–Ambolikha watershed (Table 4). These estimates suggest that during summer low-flow, ca. 20.4×10^6 g C d^{-1} is emitted as CO_2 to the atmosphere from streams and rivers in the watershed (with streams emitting ca. 17.7×10^6 g C d^{-1} and rivers—excluding the Panteleikha—emitting ca. 2.7×10^6 g C d^{-1}). However, total CO_2 emission from the watershed is reduced to ca. 11.9×10^6 g C d^{-1} when incorporating the Panteleikha (as this river acted as a sink, decreasing CO_2 evasion by ca. 8.5×10^6 g C d^{-1}). Therefore, of the CO_2 emitted to the atmosphere, streams accounted for 86%, rivers accounted for 10% and the Ambolikha main stem accounted for 4%. The Panteleikha River (during our period of observation) reduced the total estimated CO_2 evasion by 42%.

Discussion

Spatial patterns of CO_2 evasion

Streams measured in this study were consistently supersaturated in CO_2, suggesting they act as net sources of CO_2 to the atmosphere during the summer low-flow period. Larger rivers (including the Kolyma River main stem) contained relatively low CO_2, yet occasionally were supersaturated in CO_2, resulting in these water bodies acting as weak net sources and periodically weak net sinks of atmospheric CO_2. The observed gradient and magnitude of directional processing from small streams to large tributaries is consistent with findings in other

Table 3 Estimates of areal CO_2 evasion fluxes from surface waters of the northern Kolyma River bounded study area (black box in Fig. 3) during summer low-flow conditions.

Inland water type	Surface water area (km^2)	Surface water area (%)	Total study area (%)	Average pCO_2[a] (µatm)	CO_2 evasion flux (g C m^{-2} d^{-1})	Total areal CO_2 emission (10^6 g C d^{-1})	Fractional CO_2 contribution (%)
Streams ($n = 1034$)	4.2	2.4	0.2	2860	7.00	29.5	38.3
Order 1 ($n = 686$)	1.6			3137	7.78	12.1	
Order 2 ($n = 256$)	1.5			2886	7.07	10.6	
Order 3 ($n = 92$)	1.1			2556	6.14	6.7	
Small rivers ($n = 4$)	5.6	3.2	0.3	378	−0.001	0.3	0.4
Ltp	0.3			264	−0.27	−0.1	
Skotnikvo	0.9			397	0.02	0.01	
Panteleikha	2.4			145	−0.50	−1.2	
Ambolikha	2.0			707	0.75	1.5	
Large rivers ($n = 2$)	29.0	16.7	1.6	388	−0.005	−1.5	−2.0
Bolshoi A.	9.8			461	0.14	1.4	
Malinki A.	19.2			316	−0.15	−2.9	
Kolyma main stem ($n = 1$)	134.8	77.7	7.2	547	0.35	47.2	61.3
Bounded area (1871 km^2)	173.1	100	9.3	1049	2.1	75.5	98

[a]Partial pressure of carbon dioxide.

Table 4 From a watershed perspective, estimates of CO_2 evasion fluxes were scaled up to the Ambolikha–Panteleikha watershed during summer low-flow conditions.

Inland water type	Surface water area (km^2)	Surface water area (%)	Watershed area (%)	Average pCO_2 (µatm)[d]	CO_2 evasion flux (g C m^{-2} d^{-1})	Total areal CO_2 emission (10^6 g C d^{-1})[e]	Fractional CO_2 contribution (%)
Streams (order 1–3)	2.4[a]	8.7	0.13	2883	7.2	17.7	86.4
Rivers (order 4–5)	6.9[a]	24.9	0.37	456	0.3	1.9	9.5
Ambolikha River	1.1[b]	4.1	0.06	707	0.8	0.8	4.1
Panteleikha River	17.3[c]	62.3	0.93	145	−0.5	−8.5	−41.7
Panteleikha–Ambolikha watershed (1849 km^2)	27.7	100	1.49	1048	1.9	11.9	58.3

[a]The proportion of total in known 30% of watershed (yellow area in Fig. 3) was applied to the total watershed.
[b]Determined by reclassification of GeoEye imagery.
[c]Length manually measured using Orthorectified Landsat Thermatic Mapper mosaic imagery and multiplied by average width.
[d]Average partial pressure of carbon dioxide (pCO_2) from samples collected; streams ($n = 8$), rivers ($n = 3$), Ambolikha ($n = 1$) Panteleikha ($n = 4$).
[e]Positive value indicates CO_2 emitted to the atmosphere and negative value indicates CO_2 absorbed by water surfaces.

regions (Teodoru et al. 2009; Koprivnjak et al. 2010; Butman & Raymond 2011). Since small streams are tightly connected to the landscape, they receive and process terrestrially derived organic C (e.g., Vannote et al. 1980). In a study conducted by Öquist et al. (2009), 90% of DIC originating from soil was released to the atmosphere as CO_2 within 200 m of the water entering the stream, suggesting subsurface inflow of DIC is rapidly evaded from streams. Arctic streams may also function as hotspots for CO_2 evasion which is particularly important to understand as permafrost C is likely to be initially mobilized into smaller headwater streams. Additionally, factors including increased photochemical degradation and residence times as well as increased autochthonous production, flocculation and sedimentation may result in lower rates of CO_2 accumulation in larger rivers. We may therefore expect downstream river CO_2 budgets to be influenced more by in-stream processes (e.g., microbial productivity), whereas smaller stream CO_2 patterns to be primarily driven by catchment characteristics and stream morphology.

Variability in stream pCO_2 (ranging from 274 to 9402 µatm) and k (ranging from 3.2 to 54.6 cm h^{-1}), resulted in consistently high and variable CO_2 evasion rates (ranging from −0.33 to 20.56 g C m^{-2} d^{-1}). In a study by Alin et al. (2011) sensitivity analysis showed that k was particularly sensitive to changes in stream depth and water velocity, which may account for the variability in k observed here. Measured k_{600} values in this study are comparable to floating chamber values reported in the literature with average values of 24.6, 17.6, and 18.0 cm h^{-1} for streams, rivers and main stem, respectively (e.g., Vachon et al. 2010). Furthermore, Laudon et al. (2011) found that in heterogeneous catchments, the C quantity entering stream waters was regulated by a combined effect of hydrological mechanisms and the proportion of major landscape characteristics. In the northern region of the Kolyma River basin, floodplain streams on average had the highest pCO_2, whereas yedoma streams on average had the highest DOC concentrations. Furthermore, connecting streams had pCO_2 an order of magnitude lower than floodplain and yedoma streams, as lakes and wetlands draining into the stream likely process organic C before entry. It is therefore likely the lability of organic C sourced to the streams in this region differed: young C leached from floodplain vegetation throughout the growing season is generally comprised by low molecular weight, hydrophilic compounds that are rapidly biodegradable compared to more aromatic, higher molecular weight permafrost soils (e.g., Wickland et al. 2007).

Citation: *Polar Research* 2013, *32*, 19704, http://dx.doi.org/10.3402/polar.v32i0.19704

Only half of the rivers in this region were supersaturated in CO_2 (pCO_2 averaged 412 ± 250 μatm), suggesting that rivers in this region were near equilibrium with respect to atmospheric CO_2 during the summer low-flow period. Similar respiration and production rates may partially explain these observations of low pCO_2. Measurements of BOD were consistent, suggesting low, yet continuous metabolism of organic C and the generation of CO_2. The general reduction in BOD from streams to rivers is also consistent with the preferential utilization of a more labile C fraction in smaller headwaters. In addition, rivers sampled in the Kolyma River basin are meandering, relatively shallow and therefore potentially conducive to in situ primary production during this time of the year. Significant phytoplankton growth was observed in the Panteleikha River during our study period, resulting pCO_2 declining from 219 to 5 μatm. Although rivers were found to act as both a net source and a net sink of atmospheric CO_2 during summer low-flow, this may vary seasonally when light availability and hydrologic conditions change.

Our study could not differentiate the source of CO_2 production between surface and subsurface terrestrial flow paths and in situ metabolism; however, a continuous flow of C is likely being sourced to the river network via surface or subsurface flow. We therefore hypothesize that surface and subsurface flow of terrestrial organic C supported the majority of CO_2 production. During low-flow conditions, the stable surface water volume and floodplain–river connectivity is typically reduced (Battin et al. 2008), resulting in consistent subsurface flow with sporadic floodplain-river surface flow during high precipitation events. Mann et al. (2012) found evidence in the Kolyma River main stem to suggest that dominant flow paths shifted over the year from the organic surface layer during spring freshet to flow through deeper soil horizons (i.e., yedoma soils rich in organic C) via deepening of the active layer during summer. Respiration of terrestrially derived organic matter is actively occurring across fluvial paths in the Kolyma River network, as DOC and BOD had a similar decrease from headwater streams to larger rivers during the summer low-flow period. Humborg et al. (2010) found DIC increased downstream within Swedish watersheds, suggesting groundwater can regulate a continuous inflow of CO_2 within a river network. However, the Kolyma River basin has been suggested to have relatively low annual flow-weighted DIC concentrations compared to other major Arctic rivers, of which 72% is bicarbonate or carbonate (i.e., not present as CO_2; Tank et al. 2012). Rather, high DOC flux and resulting high riverine DOC concentrations in Eurasian watersheds (Holmes et al. 2012) and high inputs of particulate organic matter from coastal erosion across the Siberian coast (Vonk et al. 2012) likely contribute substantially to the source of CO_2 production in the Kolyma River basin.

Areal CO_2 emission

Area-specific CO_2 evasion fluxes from streams were an order of magnitude greater than the Kolyma main stem, but the total CO_2 emission from these sub-categories was on the same order of magnitude given that the surface area of the Kolyma main stem covers about 32 times that of streams (within our bounded study area). Conversely, streams occupy a relatively small proportion of the total study area (ca. 0.2%), yet act as hotspots for CO_2 evasion due to typically high pCO_2 and k values.

Although current studies have begun to measure stream pCO_2 at regional scales, few studies have attempted to quantify gas exchange velocities and surface areas of small streams at regional scales. Unlike larger rivers and lakes, narrow and densely vegetated streams are difficult to detect in satellite imagery (Benstead & Leigh 2012) and upscaling current gas exchange at small spatial scales is problematic due to the variation between streams and larger water bodies (Raymond et al. 2012). Even with the use of GeoEye imagery, currently the highest spatial resolution imagery publicly available for this region (ca. 0.41–1.65 m), the smallest streams measured in situ were not detected. Therefore, estimates of stream surface area, inclusion of under-represented streams (using physical characteristics as a proxy), and directly measured k unique to streams allowed for improved spatially extrapolated field-based observations. In this study, stream width had the best predictive power ($r^2 = 0.66$) for our observed pCO_2. pCO_2 was negatively exponentially related to width, whereas pCO_2 in streams declined with an increase in width. This is an expected relationship, as past studies (e.g., Hope et al. 2001) have also found pCO_2 to decline along the stream gradient.

CO_2 evasion flux estimates from this study were compared to other regions (Table 5) to assess the overall relative importance of summer CO_2 emissions from the Kolyma River basin. It is important to note that comparisons among regions should be interpreted with caution as land cover, hydrologic processes, and sampling techniques may differ between studies. From these first-order comparisons, however, it is evident that CO_2 evasion from inland waters in the northern Kolyma River basin are comparable to inland water systems typical of Northern Hemisphere regions (temperate, boreal and Alaskan Arctic). We suggest that, driven by large contributions from small streams, the Kolyma River basin could be an

Table 5 A summary of CO_2 evasion fluxes from published studies of streams, rivers and main stem locations across different geographic regions in the Northern Hemisphere. Evasion estimates were adapted from the literature to be expressed as a loss of grams of C per m^2 of water surface area per day. The selection includes studies for which daily evasion estimates were available (or could be readily calculated) for summer (June–August). CO_2 evasion fluxes are recorded as a range and/or a mean of samples.

		CO_2 evasion flux (g C m^{-2} d^{-1})			
Region	Watershed	Streams	Rivers	Main stem	Reference
Siberia	Kolyma River, Russia[a]	−0.33 to 26.56 8.59	−0.77 to 1.27 0.01	−0.62 to 1.36 0.46	This study
Arctic	North Slope, Alaska	–	0.02 to 0.15 0.09	–	Kling et al. (1991)
Boreal	Eastman River, Canada	3.12	0.39	0.19	Teodoru et al. (2009)
Temperate	Brocky Burn, Scotland	0.26 to 45.88 –	–	–	Hope et al. (2001)

[a]Calculated from all field-based samples; see Table 1.

important contributor to global inland water CO_2 emission. However, to provide this broad conclusion, annual flux estimates from the entire Kolyma River basin are required. Our findings may provide a predictive conceptual model that could be used in similar locations in the Arctic with fluvial systems underlain by permafrost.

To provide a broad estimate of the importance of C contributions from the Kolyma River basin at a watershed scale, results from the northern Kolyma River bounded study area (Fig. 3) were further scaled to the Panteleikha–Ambolikha watershed (Table 4). Extrapolating across the Panteleikha–Ambolikha watershed, our estimates suggest streams play a major role in CO_2 emission during summer low-flow, providing 86% of the total ca. 20.4×10^6 g C d^{-1} estimated for the combined watershed (whereas the Ambolikha main stem and rivers accounted for the remaining 14%). The Panteleikha River acted as a net CO_2 sink (-8.5×10^6 g C d^{-1}) reducing the total watershed CO_2 emission to ca. 11.9×10^6 g C d^{-1}. Across the watershed, rivers (order 4–5) covered about three times more surface area than streams (order 1–3), yet streams emit about nine times more CO_2 per day compared to rivers. This broad GIS-based estimate of CO_2 emission from fluvial environments within the Panteleikha–Ambolikha watershed provides valuable insights into the fractional CO_2 contribution across the whole Kolyma River basin. These results suggest that although streams cover a small proportion of total inland water surface area, their fractional atmospheric CO_2 emission is substantial. In contrast, rivers have a larger surface water area and are close to equilibrium with atmospheric CO_2, contributing much less to overall watershed CO_2 emission during the summer low-flow period.

Future implications

In this study, we were able to approximate the three terms needed to estimate areal CO_2 emission: pCO_2, k, and water surface area. Our CO_2 emission estimates capture a diverse stream and river network in the northern region of the Kolyma River basin; however, regional diversity, seasonality, and lake measurements were not captured in this study. Current findings in boreal regions suggest CO_2 evasion from streams is highest during the summer (Koprivnjak et al. 2010). However, CO_2 evasion from large rivers and the Kolyma River main stem may be highest during the spring flood pulse when floodplains and rivers are connected and young fresh C is exported (Mann et al. 2012). To prevent overestimating annual CO_2 emission from streams and underestimating annual CO_2 emission from rivers, only CO_2 evasion fluxes during summer low-flow conditions were utilized in this study. Future studies need to consider how to incorporate additional seasons to arrive at accurate annual evasion. In addition, we neglected to address the role of lakes in this study. Lakes have the potential to significantly influence regional C evasion budgets within the Kolyma River basin, as they cover about 10% of the entire watershed area (Welp et al. 2005). Utilizing empirically-measured gas exchange velocities for a set of streams and rivers in the Kolyma River basin provided a basis for producing regionally representative values that improved the accuracy of CO_2 emission estimates. Applying generalized gas transfer velocities from the literature has been found to produce an error of up to 100% in CO_2 evasion fluxes (Wallin et al. 2011). Furthermore, overestimations caused by floating chambers is not consistent and is dependent on the turbulence regime, with a strong bias found in calm, low turbulent

Citation: *Polar Research* 2013, *32*, 19704, http://dx.doi.org/10.3402/polar.v32i0.19704

(wind speed <1–2 m s^{-1}) environments (Vachon et al. 2010). Based on the overestimation ratio outlined in Vachon et al. (2010), our samples, with an average wind speed of ca. 3 m s^{-1} in rivers and an average current of ca. 15 cm s^{-1} in streams, have a mean overestimation ratio of 1.58 ± 0.34. Finally, this study used the best available remotely sensed imagery during the summer low-flow period to estimate stream and river surface areas, but as new technology and satellite imagery become available, these estimates should be refined and should also include estimates of lake surface area.

Quantification of the net emission of CO_2 from freshwater ecosystems is necessary on a global scale (Cole et al. 2007), with particular regional emphasis placed on high-latitude ecosystems susceptible to C loss via permafrost thaw (Battin et al. 2009). This study provides a starting point for estimating regional CO_2 emission by incorporating spatial variability of pCO_2 and k during summer low flow from streams to rivers and representing total areal coverage of understudied headwater streams in the Kolyma River basin. The results of this study suggest hydrological flow paths and terrestrial derived C sources are key determinants of the observed spatial variability in stream CO_2 evasion, while in situ aquatic ecosystem processes likely play more of a role in river and main stem CO_2 evasion. A more detailed characterization of C cycling in the Kolyma River basin is needed to better quantify watershed-wide CO_2 emissions and more fully understand the mechanisms that deliver and generate CO_2 in the water column and subsequent atmospheric evasion. CO_2 evasion from water surfaces within the Kolyma River basin will depend on the environmental response of the surrounding permafrost-dominated landscape, requiring a sustained watershed-level analysis of the annual transport and processing of C as it moves with water from terrestrial uplands to the Arctic Ocean. Similar efforts are required in diverse Arctic regions to best quantify CO_2 emissions from the entire Arctic Ocean watershed and accurately assess the overall contribution of Arctic inland waters to the global C budget.

Acknowledgements

The corresponding author (BAD) is now at the Limnology, Department of Ecology and Genetics, Evolutionary Biology Center, Uppsala University, Norbyvägan 18D, SE-752 36 Uppsala, Sweden. This work was supported by the National Science Foundation Arctic Sciences Division as part of the Polaris Project (www.thepolarisproject.org; grants NSF-0732586, NSF-1044560, and NSF-0732944). The authors thank Alexander Shiklomanov for providing discharge data for the Kolyma River, Suzanne Tank for providing assistance with CO_2 calculations, Emily Sturdivant for helping to collect gas exchange velocities, Matthew Salter for providing assistance with developing protocols for gas exchange velocity measurements, and Christopher Williams for providing useful feedback on previous versions of this manuscript. They are particularly grateful for Ekaterina Bulygina's expertise in helping them generate DOC, alkalinity and pH data. They finally thank Andy Bunn, Sudeep Chandra,Sergei Davydov, Anya Davydova, Travis Drake, Claire Griffin, Joanne Heslop, John Schade, Erin Seybold, Valentin Spektor, Jorien Vonk, Nikita Zimov, and Sergei Zimov for assistance with sample collection and/or project coordination. We additionally thank the Polar Geospatial Center (http://www.pgc.umn.edu/) for providing GeoEye high resolution satellite imagery.

References

Alin S.R., Rasera M., Salimon C.I., Richey J.E., Holtgrieve G.W., Krusche A.V. & Snidvongs A. 2011. Physical controls on carbon dioxide transfer velocity and evasion in low-gradient river systems and implications for regional carbon budgets. *Journal of Geophysical Research—Biogeosciences 116*, G01009, doi: 1029/2010jg001398.

Aufdenkampe A.K., Mayorga E., Raymond P.A., Melack J.M., Doney S.C., Alin S.R., Aalto R.E. & Yoo K. 2011. Riverine coupling of biogeochemical cycles between land, oceans, and atmosphere. *Frontiers in Ecology and the Environment 9*, 53–60.

Battin T.J., Kaplan L.A., Findlay S., Hopkinson C.S., Marti E., Packman A.I., Newbold J.D. & Sabater F. 2008. Biophysical controls on organic carbon evasion in fluvial networks. *Nature Geoscience 1*, 95–100.

Battin T.J., Luyssaert S., Kaplan L.A., Aufdenkampe A.K., Richter A. & Tranvik L.J. 2009. The boundless carbon cycle. *Nature Geoscience 2*, 598–600.

Benstead J.P. & Leigh D.S. 2012. An expanded role for river networks. *Nature Geoscience 5*, 578–679.

Bishop K., Buffan I., Erlandsson M., Fölster J., Laudon H., Seibert J. & Temnerud J. 2008. Aqua incognita: the unknown headwaters. *Hydrology Processes 22*, 1239–1242.

Butman D. & Raymond P.A. 2011. Significant efevasion of carbon from streams and rivers in the United States. *Nature Geoscience 4*, 839–842.

Cole J.J., Caraco N.F., Kling G.W. & Kratz T.K. 1994. Carbon dioxide supersaturation in the surface water of lakes. *Science 265*, 1658–1570.

Cole J.J., Prairie Y.T., Caraco N.F., McDowell W.H., Tranvik L.J., Striegl R.G., Duarte C.M., Kortelainen P., Downing J.A., Middelburg J.J. & Melack J. 2007. Plumbing the global carbon cycle, integrating inland waters into the terrestrial carbon budget. *Ecosystems 10*, 171–184.

Davidson E.A., Figueiredo R.O., Markewitz D. & Aufdenkampe A.K. 2010. Dissolved CO_2 in small catchment streams of eastern Amazonia, a minor pathway of terrestrial carbon loss. *Journal of Geophysical Research—Biogeosciences 115*, G04005, doi: 10.1029/2009JG00120.

Frey K.E. & McClelland J.W. 2009. Impacts of permafrost degradation on Arctic river biogeochemistry. *Hydrological Processes 23*, 169–182.

Frey K.E., Siegel D.I. & Smith L.C. 2007. Geochemistry of west Siberian streams and their potential response to permafrost degradation. *Water Resources Research 43*, W03406, doi: 10.029/2006WR004902.

Holmes R.M., McClelland J.W., Peterson B.J., Tank S.E., Bulygina E., Eglinton T.I., Gordeev V.V., Gurtovaya T.Y., Raymond P.A., Repeta D.J., Stables R., Striegl R.G., Zhulidov A.V. & Zimov S.A. 2012. Seasonal and annual fluxes of nutrients and organic matter from large rivers to the Arctic Ocean and surrounding seas. *Estuaries and Coasts 35*, 369–382.

Holmes R.M., McClelland J.W., Raymond P.A., Frazer B.B., Peterson B.J. & Stieglitz M. 2008. Lability of DOC transported by Alaskan rivers to the Arctic Ocean. *Geophysical Research Letters 35*, L03402, doi: 10.1029/2007GL032837.

Hope D., Palmer S.M., Billett M.F. & Dawson J.J.C. 2001. Carbon dioxide and methane evasion from a temperate peatland stream. *American Society of Limnology and Oceanography 46*, 847–857.

Hope D., Palmer S., Billett M.F. & Dawson J.J.C. 2004. Variations in dissolved CO_2 and CH_4 in a first order stream and catchment: an investigation of soil-stream linkages. *Hydrological Processes 18*, 3255–3275.

Humborg C., Mörth C-M., Sundbom M., Borg H., Blenckner T., Gieslers R. & Ittekkot V. 2010. CO_2 supersaturation along the aquatic conduit in Swedish watersheds as constrained by terrestrial respiration, aquatic respiration and weathering. *Global Change Biology 16*, 1966–1978.

Jones J.B., Stanley E.H. & Mulholland P.J. 2003. Long-term decline in carbon dioxide supersaturation in rivers across the contiguous United States. *Geophysical Research Letters 30*, article no. 1495, doi: 10.1029/2003GL017056.

Kelly C.A., Fee E., Ramlal P.S., Rudd J.W.M., Hesslein R.H., Anema C. & Schindler E.U. 2001. Natural variability of carbon dioxide and net epilimnetic production in the surface waters of boreal lakes of different sizes. *American Society of Limnology and Oceanography 46*, 1054–1064.

Kling G.W., Kipphut G.W. & Miller M.C. 1991. Arctic lakes and streams as gas conduits to the atmosphere: implications for tundra carbon budgets. *Science 251*, 298–301.

Koprivnjak J-F., Dillon P.J. & Molot L.A. 2010. Importance of CO_2 evasion from small boreal streams. *Global Biogeochemical Cycles 24*, GB4003, doi: 10.1029/2009GB003723.

Laudon H., Berggren M., Ågren A., Buffam I., Bishop K., Grab T., Jansson M. & Köhler S. 2011. Patterns and dynamics of dissolved organic carbon (DOC) in boreal streams: the role of processes, connectivity, and scaling. *Ecosystems 14*, 880–893.

Mann P.J., Davidova A., Zimov N., Spencer R.G.M., Davidov S., Bulygina E., Zimov S. & Holmes R.M. 2012. Controls on the composition and lability of dissolved organic matter in Siberia's Kolyma River basin. *Journal of Geophysical Research—Biogeosciences 117*, G01029, doi: 10.1029/2011JG00 1798.

Melack J. 2011. Biogeochemistry: riverine carbon dioxide release. *Nature Geoscience 4*, 821–822.

Millero F.J. 1979. The thermodynamics of the carbonate system in seawater. *Geochimica et Cosmochimica Acta 43*, 1651–1661.

Millero F.J. 2010. Carbonate constants for estuarine waters. *Marine Freshwater Research 61*, 139–142.

Neff J.C., Finlay J.C., Zimov S.A., Davudov S.P., Carrasco J.J., Schuur E.A.G. & Davydiva A.I. 2006. Seasonal changes in the age and structure of dissolved organic carbon in Siberian rivers and streams. *Geophysical Research Letters 33*, L23401, doi: 10.1029/2006GL028222.

Öquist M., Wallin M., Seibert J., Bishop K. & Laudon H. 2009. Dissolved inorganic carbon export across the soil/stream interface and its fate in a boreal headwater stream. *Environmental Science and Technology 43*, 7364–7369.

Rasera M.F.F.L., Ballester M.V.R. & Krusche A.V. 2008. Estimating the surface area of small rivers in the southwestern Amazon and their role in CO_2 outgassing. *Earth Interactions 12*, article no. 6, doi: 10.1175/2008EI257.

Raymond P.A., Zappa C.J., Butman D., Bott T.L., Potter J., Mulholland P., Laursen A.E., McDowell W.H. & Newbold D. 2012. Scaling the gas transfer velocity and hydraulic geometry in streams and small rivers. *Limnology and Oceanography 2*, 41–53.

Richey J.E., Melack J.M., Aufdenkampe A.K., Ballester V.M. & Hess L.L. 2002. Outgassing from Amazonian rivers and wetlands as a large tropical source of atmospheric CO_2. *Nature 416*, 617–620.

Semiletov I.P. 1999. Aquatic sources and sinks of CO_2 and CH_4 in the polar regions. *Journal of the Atmospheric Sciences 56*, 286–306.

Smith L.C. & Alsdorf D.E. 1998. Control on sediment and organic carbon delivery to the Arctic Ocean revealed with space-borne synthetic aperture radar: Ob' River, Siberia. *Geology 26*, 395–398.

Stumm W. & Morgan J.J. 1981. *Aquatic chemistry*. New York: John Wiley & Sons.

Tank S.E., Raymond P.A., Striegl R.G., McClelland J.W., Holmes R.M., Fiske G.J. & Peterson B.J. 2012. *Global Biogeochemical Cycles 26*, GB4081, doi: 10.1029/2011GB004 192.

Tans P. & Keeling R. Undated. Trends in atmospheric carbon dioxide. Scripps Institution of Oceanography, National Oceanic and Atmospheric Administration, Earth System Research Laboratory database. Accessed on the internet at http://www.esrl.noaa.gov/gmd/ccgg/trends/ on 14 January 2013.

Teodoru C.R., del Giorgio P.A., Prairie Y.T. & Camire M. 2009. Patterns in pCO_2 in boreal streams and rivers of northern

Quebec, Canada. *Global Biogeochemical Cycles 23*, GB2012, doi: 10.1029/2008GB003404.

Thurman E.M. 1985. *Organic geochemistry of natural waters*. Lancaster: Martinus Nijhoff/Dr. W. Junk.

Vachon D., Prairie Y.T. & Cole J.J. 2010. The relationship between near-surface turbulence and gas transfer velocity in freshwater systems and its implications for floating chambers measurements of gas exchange. *Limnology and Oceanography 55*, 1723–1732.

Vannote R.L., Minshall G.W., Cummins K.W., Sedell J.R. & Cushing C.E. 1980. The river continuum concept. *Canadian Journal of Fisheries and Aquatic Science 37*, 130–137.

Vonk J.E., Sánchez-Garcia L., van Dongen B.E., Alling V., Kosmach D., Charkin A., Semiletov I.P., Dudarev O.V., Shakhova N., Roos P., Eglinton T.I., Andersson A. & Gustafsson Ö. 2012. Activation of old carbon by erosion of coastal and subsea permafrost in Arctic Siberia. *Nature 489*, 137–140.

Wallin M., Buffam I., Öquist M., Laudon H. & Bishop K. 2010. Temporal and spatial variability of dissolved inorganic carbon in a boreal stream network, concentration and downstream evasion. *Journal of Geophysical Research—Biogeosciences 115*, GO2014, doi: 10.1029/2900JG001100.

Wallin M., Öquist M., Buffam I., Billett M., Nisell J. & Bishop K. 2011. Spatiotemporal variability of the gas transfer coefficient (K_{CO2}) in boreal streams: implications for large scale estimates of CO_2 evasion. *Global Biogeochemical Cycles 25*, GB3025, doi: 10.1029/2010GB003975.

Weiss R.F. 1974. Carbon dioxide in water and seawater: the solubility of a non-ideal gas. *Marine Chemistry 2*, 203–215.

Welp L.R., Randerson J.T., Finlay J.C., Davydov S.P., Zimova G.M., Davydova A.I. & Zimov S.A. 2005. A high-resolution time series of oxygen isotopes from the Kolyma River, implications for seasonal dynamics of discharge and watershed-scale water use. *Geophysical Research Letters 32*, L14401, doi: 10.1029/2005GL022857.

Wickland K.P., Neff J.C. & Aiken G.R. 2007. Dissolved organic carbon in Alaskan boreal forest, sources, chemical characteristics, and biodegradability. *Ecosystems 10*, 1323–1340.

Zhang T., Barry R.G., Knowles K., Heginbottom J.A. & Brown J. 1999. Statistics and characteristics of permafrost and ground-ice distribution in the Northern Hemisphere. *Polar Geography 2*, 132–154.

Zimov S.A., Schuur E.A.G. & Chapin III F.S. 2006. Permafrost and the global carbon budget. *Science 312*, 1612–1613.